

**Obese mice lacking iNOS are sensitized to the metabolic actions of PPAR $\gamma$  agonism**

Patrice Dallaire<sup>1,2</sup>, Kerstin Bellmann<sup>1,2</sup>, Mathieu Laplante<sup>1,3</sup>, Stéphanie Gélinas<sup>1,2</sup>, Carolina Centeno-Baez<sup>1,2</sup>, Patrice Penfornis<sup>1,2</sup>, Marie-Line Peyot<sup>4</sup>, Martin G. Latour<sup>4</sup>, Julien Lamontagne<sup>4</sup>, Maria E. Trujillo<sup>5</sup>, Philipp E. Scherer<sup>5,6</sup>, Marc Prentki<sup>4</sup>, Yves Deshaies<sup>1,3</sup>, and André Marette<sup>1,2</sup> \*

<sup>1</sup>Department of Anatomy and Physiology, Laval University,

<sup>2</sup>Lipid Research Unit, Laval University Hospital Research Center, and

<sup>3</sup>Laval Hospital Research Center, Québec, Québec, Canada,

<sup>4</sup>Molecular Nutrition Unit, Department of Nutrition and Biochemistry, University of Montreal and the Montreal Diabetes Research Centre, Centre Hospitalier de l'Université de Montréal, Montréal, Québec, Canada.

<sup>5</sup>Departments of Cell Biology and Medicine, Diabetes Research and Training Center, Albert Einstein College of Medicine, Bronx, New York 10461, USA.

<sup>6</sup>Touchstone Diabetes Center, Department of Internal Medicine, University of Texas Southwestern Medical Center, Dallas, Texas, 75390-8549, USA.

\*Address correspondence to:

Dr. André Marette

Department of Physiology & Lipid Research Unit

Laval University Hospital Research Center

2705, Laurier Bld

Ste-Foy, (Québec), Canada, G1V 4G2

E-mail:andre.marette@crchul.ulaval.ca

Received for publication 22 April 2008 and accepted in revised form 29 April 2008.

Additional information for this article can be found in an online appendix at

<http://diabetes.diabetesjournals.org>

*Objective:* Synthetic ligands for peroxisome proliferator-activated receptor  $\gamma$  (PPAR $\gamma$ ) improve insulin sensitivity in obesity but it is still unclear if inflammatory signals modulate their metabolic actions. In this study we tested whether targeted disruption of iNOS, a key inflammatory mediator in obesity, modulates the metabolic effects of rosiglitazone (RSG) in obese mice.

*Research Design and Methods:* iNOS<sup>-/-</sup> and iNOS<sup>+/+</sup> were subjected to a high-fat diet or standard diet for 18 weeks and were then treated with RSG for 2 weeks. Whole-body insulin sensitivity and glucose tolerance were determined and metabolic tissues harvested to assess activation of insulin and AMPK signaling pathways and the levels of inflammatory mediators.

*Results:* RSG was found to similarly improve whole-body insulin sensitivity and insulin signaling to Akt/PKB in skeletal muscle of obese iNOS<sup>-/-</sup> and obese iNOS<sup>+/+</sup> mice. However, RSG further improved glucose tolerance and liver insulin signaling only in obese mice lacking iNOS. This genotype-specific effect of RSG on glucose tolerance was linked to a markedly increased ability of the drug to raise plasma adiponectin levels. Accordingly, RSG increased AMPK activation in muscle and liver only in obese iNOS<sup>-/-</sup> mice. PPAR $\gamma$  transcriptional activity was increased in adipose tissue of iNOS<sup>-/-</sup> mice. Conversely, treatment of 3T3-L1 adipocytes with a nitric oxide donor blunted PPAR $\gamma$  activity.

*Conclusions:* Our results identify the iNOS/NO pathway as a critical modulator of PPAR $\gamma$  activation and circulating adiponectin levels, and show that invalidation of this key inflammatory mediator improves the efficacy of PPAR $\gamma$  agonism in an animal model of obesity and insulin resistance.

**P**eroxisome proliferator-activated receptor  $\gamma$  (PPAR $\gamma$ ) is a member of the ligand-activated nuclear receptor family which is highly expressed in adipose tissues where it promotes adipocyte differentiation and lipid storage. PPAR $\gamma$  can be activated by several endogenous lipid ligands and is a known target of the anti-diabetic agents thiazolidinediones (TZDs) (1). TZDs are known for their lipid lowering and insulin sensitizing actions and are currently used to manage obesity-linked insulin resistance and type 2 diabetes (2). Although the molecular mechanism of action of TZD/PPAR $\gamma$  ligands on glucose and lipid metabolism is not fully understood, their ability to increase plasma levels of adiponectin, an adipose-specific secretory protein, is thought to be involved in their metabolic and insulin sensitizing actions (3-5). Adiponectin circulates as both a hexamer and a high molecular weight (HMW) oligomer. The latter complex form mediates the effects of TZDs on insulin sensitivity, particularly on hepatic glucose production (5-8). The insulin-sensitizing activity of adiponectin appears to involve the activation of AMP-activated protein kinase (AMPK) (4; 6), a metabolic sensor that has been reported to alleviate obesity-driven insulin resistance through metabolic and gene expression effects (9).

Anti-inflammatory mechanisms may also contribute to the beneficial action of PPAR $\gamma$  activation on insulin sensitivity. Indeed, obesity is a state of abnormal inflammatory response, leading to increased production of proinflammatory cytokines which are thought to promote insulin resistance in key metabolic tissues (10; 11). Activation of PPAR $\gamma$  opposes the effects of proinflammatory cytokines such as tumor

necrosis factor- $\alpha$  (TNF $\alpha$ ), and negatively interferes with cytokine-inducible transcriptional pathways (e.g. NF- $\kappa$ B, STAT and AP-1) in adipocytes, macrophages and other vascular wall cell types (12-15). TZDs inhibit the expression of inducible nitric oxide synthase (iNOS), a key inflammatory mediator in several cell types and tissues (16; 17). iNOS expression is increased in insulin-target tissues and pancreatic islets of animal models of dietary and genetic obesity (18-20). We have previously reported that proinflammatory cytokines and the endotoxin LPS induce iNOS expression and marked NO production in L6 myocytes and isolated rat skeletal muscles, leading to defective insulin stimulation of glucose transport (21; 22). A key role for iNOS in the pathogenesis of obesity-linked insulin resistance is supported by our previous observations that targeted disruption of iNOS protects against muscle insulin resistance and improve whole-body insulin action in high-fat fed obese mice (18). More recently, iNOS disruption was also found to protect against the adverse effects of high-fat feeding on vascular insulin resistance (23) and to reduce insulin resistance in genetically obese *ob/ob* mice (24; 25). Furthermore, iNOS is induced in skeletal muscle and adipose tissues of type 2 diabetic subjects (26; 27) where its expression correlates with the occurrence of insulin resistance (27) and obesity (26).

Whereas TZD-mediated PPAR $\gamma$  activation reduces iNOS expression in several tissues, there is also evidence suggesting that activation of the iNOS/NO pathway can blunt PPAR $\gamma$  activation. Indeed, Shibuya et al. (28) have shown that peroxynitrite, an oxidative NO derivative, inhibits ligand-dependent nuclear

translocation of PPAR $\gamma$  in macrophages, possibly through peroxynitrite-mediated nitration of PPAR $\gamma$ . This suggests that the iNOS/NO pathway modulates PPAR $\gamma$  activity, at least in myeloid cells. However, the potential role of the iNOS/NO pathway in the modulation of TZD/PPAR $\gamma$  action in key insulin target tissues of an animal model of obesity and iNOS induction has not yet been investigated. Here we have tested the hypothesis that iNOS modulates PPAR $\gamma$  activity in insulin target tissues by investigating the metabolic and gluco-regulatory effects of the TZD rosiglitazone (RSG) in both wild-type and iNOS-deficient obese mice. The results identify iNOS as a critical modulator of TZD actions in obesity.

## **MATERIALS AND METHODS**

### ***Antibodies***

Rabbit polyclonal antibodies against P-Ser473 Akt, P-Ser79 acetyl-CoA carboxylase and P-Thr172-AMPK were purchased from Cell Signaling Technology (Beverly, MA), and were used at a 1:500, 1:1000 and 1:1000 dilutions, respectively. Rabbit polyclonal iNOS, p85 and IRS-2 antibodies and rabbit monoclonal P-Ser82-PPAR $\gamma$  antibody were purchased from Upstate Biotechnology (Lake Placid, NY) and were used at a 1:500, 1:1000, 1:1000 and 1:1000 dilution, respectively. Rabbit polyclonal adiponectin antibody was used as previously described (4; 29). Mouse monoclonal PPAR $\gamma$  and P-Tyr (PY20) antibodies were purchased from Santa Cruz (Santa Cruz, CA) and used at 1:1000 dilution. Mouse monoclonal  $\alpha$ -Tubulin antibody was from Sigma (St-Louis, MO). Rabbit anti-RFP antibody (Rockland, Gilbertsville, PA) was used at 1:10000. Goat anti-mouse IgG and goat anti-rabbit IgG secondary antibodies were purchased from

GE Healthcare (Baie d'Urfé, QC, Canada) and used at a 1:10000 dilution.

### ***Animals and treatment***

This study was approved by the Animal Care and Handling Committee of Laval University. Breeding pairs of iNOS wild type mice (C57BL/6J) and iNOS knockout mice (C57BL/6-NOS2<sup>tm1Lau</sup>) were purchased from Jackson Labs (Bar Harbor, Maine, USA). Four week-old mice were fed either a ground autoclaved standard chow diet (Sterilizable Global Rodent; Harlan Teklad, Madison, Wisconsin, USA), or an irradiated high fat diet (55% of calories derived from fat) (Mouse 9F; Test Diet, Oakville, Ontario, Canada) for 18 weeks. Half of the mice in each dietary cohort were then randomly assigned to a 15-day treatment with RSG (Avandia®, GlaxoSmithKline, 30 mg/kg diet as a food admixture), corresponding to 0.1 mg per mouse per day. This dose of RSG is relatively low as compared to most studies (0.4-3 mg/day) as it was designed to test for potential sensitization of RSG effects by iNOS gene disruption.

### ***Glucose and insulin tolerance test***

Twelve days after the beginning of RSG treatment, mice were fasted at 8:00 am for 5 h and were injected with glucose (1 g/kg i.p.) or regular human insulin (Humulin® R, Lilly; 1.5 U/kg i.p.). Blood samples were collected from the tail vein at time 0 (prior to injection), 15, 30, 60, and 90 minutes after glucose or insulin injection, and blood glucose level was estimated with an Elite glucometer (Bayer, Etobicoke, Ontario, Canada).

### ***Indirect calorimetry and body composition determinations***

A subset of randomly selected mice of each group (n=6 per group) were individually monitored to determine oxygen consumption (VO<sub>2</sub>), carbon dioxide production (VCO<sub>2</sub>) and the respiratory quotient (RQ) by indirect

calorimetry. Mice were initially placed in their individual metabolic cage for 2 days before the beginning of the experiment. Measurements were made continuously during the following 2 days (36 measurements/mouse/day) in an open circuit system with an oxygen analyzer (Applied Electrochemistry, S-3A1) and a carbon dioxide analyzer (Applied Electrochemistry, CD-3A). Data presented are the average of all measurements made over 2 days of monitoring. Dual X-ray absorptiometry (DEXA) (Piximus, LUNAR Corporation, Madison, WI) was used to measure total fat and lean masses in mice anesthetized with isoflurane.

#### ***Acute insulin injection and sacrifice***

Mice were anesthetized with isoflurane and blood sampling (150-200  $\mu$ l) from the orbital sinus was performed for later plasma analysis. An acute injection of insulin (Humulin® R, Lilly; 3.8 U/kg i.v.) was then performed in the tail vein and mice were sacrificed by decapitation 4 min post-injection. Tissues were then rapidly excised and were frozen in liquid nitrogen. Blood was collected and centrifuged at 3,000 $\times$ g for 10 min at 4°C to isolate plasma. Plasma and tissues were stored at -80°C until biochemical analysis.

#### ***Islet isolation and insulin secretion measurements***

Pancreatic islets were harvested and cultured for 2 h prior initiating insulin secretion as described previously (30). Briefly, islets were distributed in batches of 10 with 4 replicates for each condition per genotype. Islets were washed and pre-incubated for 45 min at 37°C in Krebs-Ringer bicarbonate buffer containing 10 mM HEPES (KRBH, pH 7.4) with 0.5% defatted BSA (Sigma) and 3 mM glucose. The islets were then incubated for 1 h at 37°C in KRBH containing 3, 8 or 16 mM glucose and 0.5%

BSA. Some experiments were also performed in the absence or presence of 0.4 mM palmitate during the incubation. At the end of the incubation, media were withdrawn for insulin determination, and islets were harvested for assessment of total insulin content (30).

#### ***Adipose tissue histology***

Tissues were fixed in 10% buffered formalin and embedded in paraffin. Multiple 10  $\mu$ m sections were obtained from epididymal white adipose tissue (WAT) and stained with hematoxylin/eosin. Images were acquired using a BX60 microscope (Olympus, NY) and an RT slider 2.3.0 camera (Diagnostic Instrument Inc., Sterling Heights, MI, USA), and were analyzed using SPOT 4.0.2 software. For each group (n=6), at least 4 fields, representing 300 adipocytes per slide, were analyzed, and the geometric mean of adipocyte diameter was calculated to estimate adipocyte mass. Cellularity was calculated as the ratio of epididymal tissue mass/mean adipocyte mass.

#### ***RNA extraction and RT-PCR***

Fifty mg of WAT was used to isolate total RNA using Trizol Reagent (Invitrogen) and iNOS and  $\beta$ -Actin mRNAs were measured by semi-quantitative RT-PCR (18; 21). 50 ng of each of the following primer pairs was used for PCR: iNOS, 5'-CAG CCT CAG AGT CCT TCA TG-3' (forward), 5'-GGT GCT TGC CTT ATA CTG GTC-3' (reverse);  $\beta$ -Actin, 5'-TCA CCC ACA CTG TGC CCA TCT ACG A-3' (forward), 5'-GGA TGC CAC AGG ATT CCA TAC CCA-3' (reverse). Amplification products were run in 8% acrylamide gel or 1.5% agarose gel containing ethidium bromide (1  $\mu$ g/ml) and analysed under U.V. illumination.

#### ***Protein extraction, immunoprecipitation and western blotting***

Fifty mg of quadriceps muscle, WAT and liver tissues were pulverized with a pestle and mortar in liquid nitrogen and the powder was homogenized in 6 vol (muscle and liver) or 4 vol (WAT) of homogenization buffer (20 mM Tris-HCl pH 7.5, 150 mM NaCl, 1 mM CaCl<sub>2</sub>, 1 mM MgCl<sub>2</sub>, 10% glycerol, 1% Igepal CA-630, 10 mM NaF, 2 mM Na<sub>3</sub>VO<sub>4</sub>, 1 mM PMSF, and protease inhibitors). One mg of proteins were immunoprecipitated o.n. at 4°C with 2  $\mu$ g of PY20. Immune complexes were washed 3 times with PBS containing 1% NP-40, 10 mM NaF, 2 mM Na<sub>3</sub>VO<sub>4</sub> and protease inhibitors. For western blot analysis 10 to 50  $\mu$ g of crude protein lysates or immune complexes were solubilized in sample buffer and loaded on a 7.5% acrylamide gel and subjected to SDS-PAGE and western blotting as previously described (21; 22). Bands were detected by standard chemiluminescence (Perkin Elmer) and were scanned for quantification using Image J software. Adipose tissue lysates were analyzed for tumor necrosis factor (TNF)- $\alpha$  and interleukin-6 (IL-6) content using a murine ELISA kit (BD Biosciences, Mississauga, ON).

#### ***Plasma hormones and adipokines***

Plasma leptin, insulin, adiponectin and resistin levels were determined using mouse radioimmunoassay kits as recommended by the manufacturer (Linco Research, St. Charles, MO). Insulin levels during GTT were determined using a mammal ELISA kit (Alpco Diagnostics, Salem, NH). Different molecular weight adiponectin complexes were separated by velocity sedimentation / gel filtration chromatography as previously described (5; 7).

#### ***PPAR $\gamma$ expression, phosphorylation and transcriptional activity***

3T3-L1 cells, kindly provided by Dr. A Klip (Hopsital for Sick children, Toronto,

Canada) were grown and differentiated as previously described (17). Fully differentiated 3T3-L1 adipocytes were treated with sodium nitroprusside (Sigma) or peroxyntirite (Upstate) for 24 h. Cell culture supernatants were collected and nitrite levels were determined as an indirect measurement of nitric oxide production by the Griess method (17; 21; 22). Cell lysates were used for determination of PPAR $\gamma$  expression and Ser-82 phosphorylation. Nuclear extracts were prepared and 10  $\mu$ l were analysed for PPAR $\gamma$  specific transcription factor binding activity as described by the manufacturer (Cayman, Ann Arbor, MI). In brief, nuclear extracts were loaded on a 96-well plate coated with a double stranded DNA sequence containing the peroxisome proliferator response element. After 16 h incubation at 4°C the plates were washed and a primary antibody directed against PPAR $\gamma$  was added for 1 h at RT. A secondary antibody conjugated to HRP was added to provide a sensitive colorimetric readout at 450 nm. The results were corrected for total protein content in 10  $\mu$ l of nuclear extract.

HEK293T cells were kindly provided by Dr. J. Lavoie (Centre de recherche en cancérologie, Québec, Canada). The cells were transfected with mouse PPAR $\gamma$ 2 and pGL3-PPRE (kindly provided by Dr. F. Picard, Hopital Laval, Québec, Canada) and pmRFP-N1 (kindly provided by Dr. J. Lavoie) using calcium-phosphate. Twenty-four hours after transfection, cells were treated with sodium nitroprusside or peroxyntirite for 8 h followed by addition of troglitazone (20  $\mu$ M) for 16 h. Cell lysates were analyzed for luciferase activity and corrected for expression of RFP by Western blot by scanning and quantification.

#### ***Data presentation and statistical analysis***

Data are expressed as means  $\pm$  S.E. Except for basal physiological parameters, only data from the high fat diet cohorts and the chow-fed untreated iNOS<sup>+/+</sup> group (used as a reference) are shown in figures, as iNOS gene disruption and RSG treatments had only marginal effects in the chow-fed groups. The main effect of diet on all parameters were analyzed by a 2 x 2 x 2 factorial ANOVA test. The main and interactive effects of genotype (iNOS<sup>+/+</sup>, iNOS<sup>-/-</sup>) and treatment (untreated, RSG) were analyzed separately for each dietary cohort by a 2 x 2 factorial ANOVA test. All parameters of each dietary cohort were also analyzed separately by ANOVA. Pairwise between-group differences were identified in the high fat-fed cohort by post-hoc Fisher's Protected Least Significant Difference (PLSD) test. Results of the latter analysis in the high fat-fed cohort are presented at the end of each figure legend. The level of significance was chosen as  $P < 0.05$ .

## RESULTS

***Effects of genotype, high fat-feeding and RSG on physiological parameters.*** iNOS<sup>+/+</sup> and iNOS<sup>-/-</sup> mice were fed a standard low-fat chow diet or a high fat diet for 18 weeks to induce obesity and insulin resistance. Half of the mice of each dietary cohort were then treated with RSG for 15 days. High fat-fed mice of either genotype showed a similar increase in total body weight, body weight gain and total body fat mass, and RSG treatment did not affect these parameters (Table 1). The daily caloric intake of high fat-fed mice was, as expected, higher than that of chow-fed mice. A small increase in caloric intake was also observed in iNOS knockout mice ( $P = 0.03$  for genotype effect) but food consumption was similar between iNOS<sup>+/+</sup> and iNOS<sup>-/-</sup> mice during RSG treatment (Table 1).

***RSG inhibits iNOS induction in adipose tissue of obese high fat-fed mice.*** We have previously shown that iNOS is induced in high-fat fed obese mice (18). iNOS induction in white adipose tissue (WAT) of high fat-fed mice was confirmed by RT-PCR and western blot analysis of WAT (Fig. 1). We found that both iNOS mRNA and protein levels were increased 2-3 fold ( $P < 0.05$ ) in WAT of obese iNOS<sup>+/+</sup> mice compared with control chow-fed mice. RSG treatment completely normalized iNOS expression levels to those observed in chow-fed mice. As expected, iNOS expression was not detected in WAT of iNOS<sup>-/-</sup> mice.

***iNOS disruption sensitizes obese mice to the beneficial effect of RSG on glucose tolerance.*** After 18 weeks of high fat feeding, fasting blood glucose and insulin levels were increased in both obese iNOS<sup>+/+</sup> and iNOS<sup>-/-</sup> mice compared with their lean chow-fed counterparts (Table 1). RSG was found to reduce hyperglycemia in obese mice of both genotypes. Hyperinsulinemia was decreased by RSG in obese iNOS<sup>+/+</sup>, but not in obese iNOS<sup>-/-</sup> mice, as iNOS disruption per se tended to reduce insulin levels ( $P = 0.08$ ). A significant effect of iNOS gene disruption was also observed on plasma leptin and triglyceride levels (2 x 2 ANOVA test).

The effect of RSG on whole-body insulin sensitivity and glucose tolerance was next examined in both genotypes. High fat feeding caused insulin resistance and glucose intolerance in obese iNOS<sup>+/+</sup> mice compared with lean chow-fed iNOS<sup>+/+</sup> mice (Fig. 2a-d). Insulin sensitivity was independently improved by both iNOS disruption and RSG treatment as revealed by insulin tolerance curves (Fig. 2a) and the average reduction in blood glucose 15 min after insulin injection (Fig. 2b). RSG failed to further enhance insulin sensitivity in obese iNOS<sup>-/-</sup> mice. In contrast, neither

iNOS disruption nor RSG treatment alone was found to protect mice from high fat-induced glucose intolerance (Fig. 2c-d). However, RSG markedly improved glucose tolerance in obese mice lacking iNOS (Fig. 2c-d). Insulin levels during the glucose tolerance test was elevated in high-fat fed iNOS<sup>+/+</sup> and iNOS<sup>-/-</sup> mice compared with the chow-fed group (Fig. 2e). RSG reduced insulin levels ( $P < 0.05$ ) but not when combined with iNOS gene disruption. Glucose-stimulated insulin secretion (GSIS) in freshly isolated islets was increased ( $P < 0.05$ ) in high fat-fed obese iNOS<sup>+/+</sup> mice compared with islets from lean chow fed iNOS<sup>+/+</sup> mice (Fig. 2f). This effect was only observed at the highest dose of glucose tested. GSIS was affected neither by iNOS genetic deletion nor by RSG treatment. GSIS by isolated islets was also similar in the presence of palmitate during the incubations (data not shown).

***iNOS disruption increases insulin signaling to Akt/PKB in liver of RSG-treated obese mice.*** The effect of RSG on insulin action in skeletal muscle and liver of iNOS<sup>+/+</sup> and iNOS<sup>-/-</sup> mice was then assessed by measurement of insulin-mediated Ser473 phosphorylation of Akt/PKB, a key effector of insulin-induced inhibition of hepatic glucose production and stimulation of muscle glucose uptake (31). As depicted in Fig. 3, high fat feeding caused a profound insulin resistance in muscle (Fig. 3a) and liver (Fig. 3b) as demonstrated by a 50% and 75% reduction in insulin-stimulated Akt/PKB phosphorylation, respectively, compared with the effect of insulin in chow-fed mice (dashed lines). As previously observed for whole-body insulin sensitivity (insulin tolerance test), RSG treatment and iNOS deficiency both independently corrected defective insulin-induced Akt/PKB activation in muscle, but their combination did not further increase insulin

action in that tissue (Fig. 3a). Conversely, in liver, neither RSG nor iNOS gene disruption alone was found to improve insulin-stimulated Akt/PKB phosphorylation whereas RSG treatment in obese iNOS<sup>-/-</sup> markedly enhanced the ability of insulin to phosphorylate the enzyme (Fig. 3b). Similar data were obtained when assessing more proximal insulin signaling events such as insulin-induced p85 binding to tyrosine phosphorylated IRS 1/2 in muscle and liver, as well as IRS-2 tyrosine phosphorylation in liver (supplementary Fig. 1).

***iNOS disruption increases the ability of RSG to raise plasma adiponectin levels in obese mice.*** TZDs are known to exert their beneficial effects largely by increasing adiponectin circulating concentrations(4; 6). We thus next examined whether iNOS disruption modulates the ability of RSG to increase plasma adiponectin concentration in obese mice. As shown in Fig. 4a, RSG treatment induced a 2.9-fold increase in total plasma adiponectin levels in obese iNOS<sup>+/+</sup> compared with untreated obese iNOS<sup>+/+</sup> mice. A similar effect of the TZD was observed in chow-fed control mice (data not shown). Remarkably, the effect of RSG on adiponectin levels was markedly enhanced in obese iNOS<sup>-/-</sup> mice relative to obese iNOS<sup>+/+</sup> mice, as reflected by the 5.6-fold increase in the adipokine plasma concentrations following TZD treatment in the former group. Resistin plasma levels were also measured but found not to be affected by the genotype or RSG treatment (Suppl. Fig. 2a).

Since complex distribution, not the absolute amounts of adiponectin, correlates with TZD-mediated improvement in insulin sensitivity (7), we next evaluated the effect of RSG on the formation of HMW complexes of adiponectin in wild-type and iNOS-deficient animals. Obesity in both genotypes had no effect on basal HMW

adiponectin plasma levels as compared with lean control mice (Fig. 4a, dashed line). RSG barely increased HMW adiponectin in *iNOS*<sup>+/+</sup> mice but the TZD was much more potent in *iNOS*<sup>-/-</sup> mice, increasing HMW adiponectin levels by 8.2-fold in these mice. ***RSG induces adipose tissue remodeling in obese mice lacking iNOS.*** As adiponectin secretion is greater in newly differentiated small adipocytes, we next explored the possibility that RSG exerted a genotype-specific effect on adipose tissue remodeling. Histological analysis showed that RSG, at the low dose used, failed to significantly affect adipocyte size or number in obese *iNOS*<sup>+/+</sup> mice (Fig. 4b). In marked contrast, the TZD clearly induced adipose tissue remodeling in obese *iNOS*<sup>-/-</sup> mice, which was characterized by the presence of an increased number (+75%,  $P < 0.05$ ) of smaller (-45%,  $P < 0.05$ ) adipocytes compared with untreated obese *iNOS*<sup>-/-</sup> mice.

Adipose tissue levels of both TNF- $\alpha$  and IL-6 were increased by high-fat feeding in both genotypes (suppl. Fig. 2b-c). Moreover, TNF- $\alpha$  was slightly increased by RSG treatment in obese wild-type mice. Interestingly, the effect of RSG on adipose TNF- $\alpha$  levels was not observed in *iNOS*<sup>-/-</sup> mice suggesting that iNOS may be needed for this action. No effect of the genotype was observed on adipose IL-6 levels.

***Increased AMPK activation and energy expenditure in RSG-treated obese iNOS<sup>-/-</sup> mice.*** Because adiponectin activates AMPK in several tissues (32; 33), we next determined whether elevation of circulating adiponectin in response to RSG is associated with AMPK activation in insulin-target tissues. Both phosphorylation of AMPK on Thr172 and of acetyl-CoA carboxylase (ACC) on serine 79, a well-established downstream target of AMPK activation (34),

were determined (Fig. 5a-c). Activation of the AMPK pathway was found to be reduced in muscle, liver, and WAT of high-fat fed obese *iNOS*<sup>+/+</sup> mice compared with lean chow-fed *iNOS*<sup>+/+</sup> mice (dashed lines, Fig. 5a-c). At the low dose used, RSG treatment of obese *iNOS*<sup>+/+</sup> mice improved ACC phosphorylation in WAT but not in muscle and liver. However, the TZD markedly improved ACC phosphorylation in muscle, liver and WAT of mice lacking iNOS. Interestingly, the enhanced ACC phosphorylation in both liver and fat (but not in muscle) was at least partly accounted for by an increased expression of ACC, especially in *iNOS*<sup>-/-</sup> tissues. This effect of RSG to increase ACC protein levels has been recently reported in adipose tissue of high-fat fed rats (35). As AMPK activation switches on catabolic pathways and increases energy expenditure, we next determined whether enhanced activation of this pathway in RSG-treated obese *iNOS*<sup>-/-</sup> led to increased whole-body energy expenditure as measured by indirect calorimetry. As depicted in Fig. 5d, total energy expenditure was similar in untreated obese *iNOS*<sup>+/+</sup> and obese *iNOS*<sup>-/-</sup> mice. However, energy expenditure was significantly increased in obese *iNOS*<sup>-/-</sup> mice treated with RSG. The RQ was reduced in all high fat-fed groups compared with chow-fed *iNOS*<sup>+/+</sup> animals (Fig. 5d), consistent with increased consumption of dietary lipids. On the other hand, neither iNOS gene disruption nor RSG treatment of high fat-fed obese mice affected the RQ, indicating that fat remained the principal substrate source in all groups consuming the high-fat diet.

***iNOS inhibits PPAR $\gamma$  activity in adipose tissue and adipocytes.*** Since RSG action was potentiated in mice with iNOS gene disruption we next tested whether PPAR $\gamma$

activation was affected by the genotype. PPAR $\gamma$  expression was increased in chow-fed iNOS<sup>-/-</sup> mice as compared to their wild-type controls (Fig. 6a). This genotype effect was not observed in the high-fat fed mice. We also assessed PPAR $\gamma$  phosphorylation on Ser-82/112, which inhibits its transcriptional activity (36; 37). We found that PPAR $\gamma$  phosphorylation on Ser-82/112, corrected for the PPAR $\gamma$  protein abundance in the sample, was significantly reduced in adipose tissue of both chow and high-fat fed iNOS<sup>-/-</sup> mice as compared to iNOS<sup>+/+</sup> counterparts. This effect was similar for PPAR $\gamma$ 1 (Ser-82) and PPAR $\gamma$ 2 (Ser-112) isoforms which are both expressed in adipose tissue. This suggests that iNOS lack increases PPAR $\gamma$  transcriptional activity in adipose tissue. To more directly test this hypothesis, we next determined the effect of NO on PPAR $\gamma$  in cultured adipocytes. Differentiated 3T3-L1 adipocytes were exposed to increasing concentrations of the NO donor sodium nitroprusside (SNP) for 24 hrs and nitrite accumulation (Fig. 6c and d), an index of NO production) as well as PPAR $\gamma$  expression and phosphorylation were assessed by western blot analysis (Fig. 6b). These experiments revealed that SNP reduces the expression of PPAR $\gamma$  (both  $\gamma$ 1 and  $\gamma$ 2 isoforms). Furthermore, the ratio of Ser-82/112 phosphorylated PPAR $\gamma$  over total PPAR $\gamma$  protein was increased suggesting that SNP blunts PPAR $\gamma$  transcriptional activity both by lowering its expression and increasing its inhibitory phosphorylation. Interestingly, these effects were not observed upon exposing cells to the NO derivative peroxynitrite. To more directly test whether NO inhibits PPAR $\gamma$  transcriptional activity, we prepared nuclear extracts from these cells to assess PPAR $\gamma$  transcription factor binding (Fig. 6c). We also transfected HEK293T cells with a

PPAR $\gamma$  reporter (pGL3-PPRE) and looked at its troglitazone-induced activity following treatment with the NO donor SNP or peroxynitrite (Fig. 6d). These experiments revealed that SNP causes a dose-dependent inhibition of both PPAR $\gamma$  binding as well as TZD-induced activity confirming that NO but not peroxynitrite blunts PPAR $\gamma$  activity in adipocytes.

## DISCUSSION

PPAR $\gamma$  agonists such as TZDs are known for their anti-diabetic and insulin sensitizing properties. RSG and pioglitazone are two clinically approved TZDs for the management of obesity-linked type 2 diabetes but some side effects are associated with their utilization. Treatment with TZDs is usually correlated with increased body weight gain due to differentiation of fat cells as well as fluid retention caused by accelerated sodium absorption by the collecting duct (38; 39). TZD treatment has also been recently associated with increased risk for myocardial infarction and heart failure (40). This prompts the elaboration of new PPAR $\gamma$  agonists and the search for novel PPAR $\gamma$  regulatory pathways. Here we show that the iNOS/NO pathway is a novel and critical modulator of TZD/PPAR $\gamma$  action in an animal model of obesity.

To demonstrate the involvement of the iNOS/NO pathway in TZD action in vivo, we compared the action of a low dose of RSG on several gluco-regulatory and metabolic parameters in wild-type and iNOS knockout mice rendered obese by feeding a high fat diet. A relatively low dose of RSG (0.1 vs 0.4-3 mg/day in most studies (41-44)) and a short duration of treatment was used to better appreciate the effect of the absence of iNOS on the metabolic actions of TZD. We found that this low dose of RSG improves insulin sensitivity and insulin

signaling in muscle but failed to improve glucose tolerance and liver insulin signaling in wild-type obese mice. This is consistent with previous observations showing that muscle insulin sensitivity is rapidly improved by TZDs, whereas a longer duration of treatment is generally required to improve insulin action in liver (45). Recent studies using tissue-specific disruption of PPAR $\gamma$  have dissected out the contribution of the principal PPAR $\gamma$ -expressing tissues to TZD's action. Muscle PPAR $\gamma$  plays a crucial role in maintaining systemic insulin sensitivity and in mediating TZD action in muscle but not in liver (46). In contrast, liver PPAR $\gamma$  expression is not required for TZD action (47) but studies using A-Zip mice lacking adipose tissue showed TZD resistance in liver (48). Taken together, these studies suggest that the beneficial effects of TZD on the liver are most likely mediated by adipose tissue, which predominantly expresses PPAR $\gamma$  (49; 50). In agreement with these observations, the lack of significant effect of a low dose of RSG on liver insulin signaling and glucose tolerance in the present study was associated with failure of the TZD to change adipose tissue morphology. In sharp contrast, iNOS disruption was found to sensitize obese mice to the action of RSG on glucose tolerance and liver insulin action without any further effect in muscle. This genotype-specific action of TZD was linked to fat remodeling in iNOS-deficient mice as revealed by increased adipose tissue cellularity, an established indicator of adipose PPAR $\gamma$  activation (51).

It is well known that PPAR $\gamma$  agonists increase total plasma adiponectin levels by 2-3-fold (3). Adiponectin is thought to be the principal mediator of PPAR $\gamma$ 's insulin-sensitizing action. Indeed, transgene-induced overexpression of adiponectin, which raises

the secretion of the adipokine in its native oligomeric form by 3-fold, was found to induce effects similar to those of a chronic treatment with PPAR $\gamma$  agonists (4). More direct evidence for adiponectin's role in TZD action was recently provided using adiponectin null mice. Indeed, the ability of RSG to improve glucose tolerance in *ob/ob* mice lacking adiponectin is markedly diminished. Furthermore, RSG failed to activate AMPK in tissues of adiponectin null mice (6). Moreover, it has been shown that the HMW complex structure of adiponectin is key to its insulin sensitizing action, particularly in liver (7; 8). These studies showed that only HMW adiponectin can reduce blood glucose levels when injected into adiponectin-deficient mice. Consistent with these observations, only mice lacking iNOS, which showed a marked elevation in plasma HMW adiponectin levels, exhibited improved glucose tolerance and liver insulin action in response to RSG, confirming the high sensitivity of the liver to changes in HMW form concentrations (7). Adipose tissue remodeling caused by RSG treatment of iNOS knockout mice likely explains the raised plasma HMW adiponectin complexes in these animals as previous studies reported a strong inverse relationship between adipose cell size and adiponectin secretion (52; 53).

RSG treatment increased AMPK activity in fat but not in muscle and liver of wild-type obese mice even though the PPAR $\gamma$  agonist induced a 3-fold increase in plasma adiponectin levels. At first sight this may appear surprising as activation of AMPK by adiponectin is thought to be involved in its glucose metabolic and insulin-sensitizing actions (32; 33). However, this may be explained by the failure of RSG to raise plasma adiponectin in its HMW form in wild-type obese mice. Indeed, Kobayashi et

al. (54) showed that only the HMW complex of adiponectin can activate AMPK in endothelial cells. The lack of effect of RSG on HMW adiponectin secretion could be linked to iNOS induction in these animals (see Fig. 1). We propose that in iNOS-deficient obese mice, the effects of RSG on HMW adiponectin secretion and AMPK activation are unopposed by iNOS-derived NO, resulting in improved metabolic actions, as reflected by enhanced energy expenditure and decreased levels of plasma triglycerides. The finding of unaltered RQ values among the high fat-fed obese iNOS<sup>+/+</sup> and iNOS<sup>-/-</sup> groups probably reflects the fact that both fat and glucose oxidation are expected to be increased upon marked activation of AMPK in RSG-treated iNOS<sup>-/-</sup> mice. Hence, our data are consistent with the hypothesis that induction of the iNOS/NO pathway in adipose tissue of obese mice contributes to deteriorate hepatic insulin action and glucose tolerance by interfering with the ability of RSG to increase plasma HMW adiponectin and liver AMPK activation.

We further explored whether the iNOS/NO pathway blunts TZD's action by interfering with PPAR $\gamma$  transcriptional activity. Phosphorylation of PPAR $\gamma$  on Ser-82/112 is known to suppress its transcriptional activity (36; 37). Inhibitory phosphorylation of both PPAR $\gamma$  isoforms on Ser-82/112 was reduced in adipose tissue of iNOS<sup>-/-</sup> mice whereas treatment of adipocytes with the NO donor SNP enhanced PPAR $\gamma$  Ser-82/112 phosphorylation and blunted TZD-induced PPAR $\gamma$  reporter activity, consistent with the hypothesis that iNOS-derived NO represses PPAR $\gamma$  transcriptional activity. Our data further suggest that iNOS represses adipose PPAR $\gamma$  expression. This finding was not observed in high-fat fed obese mice lacking

iNOS suggesting that other factors than NO may repress PPAR $\gamma$  in adipose tissue of these obese mice.

NO exerts its action in part by inducing post-translational modifications of specific amino acid residues within target proteins. S-nitrosylation of cysteine residues within signaling proteins occurs in physiological conditions, whereas tyrosine nitration is typically associated with increased generation of the NO derivative peroxynitrite in oxidative stress-related diseases. Shibuya and co-workers previously reported that treatment of macrophages with inflammatory cytokines, LPS or peroxynitrite increased tyrosine nitration of PPAR $\gamma$  resulting in impaired ligand-dependent nuclear translocation (28). However, peroxynitrite failed to reduce PPAR $\gamma$  transcriptional activity in our adipocyte studies, suggesting that PPAR $\gamma$  regulation may be differently controlled in adipose vs myeloid cells. Further studies will be required to identify the mechanism(s) by which NO suppresses PPAR $\gamma$  activity.

We have reported that iNOS induction is repressed following AMPK activation by PPAR $\gamma$  agonists in 3T3-L1 adipocytes (17). The present study confirms that this inhibitory effect of PPAR $\gamma$  on iNOS induction also occurs in fat tissue of TZD-treated obese mice. We hypothesize that the inhibitory effect of RSG treatment on iNOS induction may be linked to its ability to raise adiponectin levels since the adipokine suppresses cytokine production and NF- $\kappa$ B transcriptional activation by activated macrophages (55; 56). However, we found that RSG treatment of wild-type mice, despite raising adiponectin levels, failed to reduce IL-6 and in fact slightly increased TNF- $\alpha$  levels in adipose tissue. This intriguing effect of RSG has been reported

previously (57). Interestingly, RSG failed to increase adipose TNF- $\alpha$  levels in iNOS-deficient mice, possibly because the drug further raised plasma adiponectin concentrations, particularly in its HMW form, thus blunting RSG effect on TNF- $\alpha$  in the latter genotype. Thus iNOS inhibition by PPAR $\gamma$  activation is a key anti-inflammatory mechanism that likely contributes to the beneficial effects of TZD in obese mice. This is exemplified by our data in iNOS-deficient mice where complete lack of iNOS was found to markedly sensitize PPAR $\gamma$  agonism in WAT, as reflected by adipose tissue histology and adiponectin secretion, particularly in its HMW form.

Taken together, our results allow the design of a model that integrates the metabolic and anti-inflammatory effects of TZD in obesity, emphasizing the roles of PPAR $\gamma$ , iNOS, adiponectin and AMPK (Fig. 7). iNOS is induced in obesity, which leads to the development of inflammation-mediated insulin resistance in skeletal muscle (18) and reduced action of PPAR $\gamma$  ligands in adipose tissue. The latter results in reduced adiponectin secretion, particularly in its HMW form, and limited activation of AMPK and tissue insulin signaling, particularly in the liver. TZD increase muscle insulin action by directly targeting muscle PPAR $\gamma$ . Lack of iNOS improved insulin sensitivity in muscle but had no effect on the liver, as we previously reported (18). However iNOS disruption sensitizes adipose tissue to PPAR $\gamma$  agonism, thus raising plasma HMW adiponectin levels. This leads to increased AMPK activation in the liver and improvement of hepatic insulin sensitivity and glucose tolerance in obese iNOS<sup>-/-</sup> mice.

The present results have potential clinical relevance. iNOS might represent a

promising therapeutic target to increase PPAR $\gamma$  agonism in obese insulin-resistant subjects, reducing the effective doses of TZDs for improving glucose tolerance. By increasing the efficacy of TZDs, iNOS inhibitors might limit the side effects of these drugs on the renal and cardiovascular systems. It has been reported that the endothelial hyperpermeability response to RSG was most pronounced at concentrations of the TZD (10–100  $\mu$ M) that correspond to the upper range of therapeutic plasma drug concentrations in routine clinical practice (58). Thus, combination therapy with low-dose of TZD and iNOS inhibitors may represent a promising avenue for the treatment of obesity-linked type 2 diabetes.

#### ACKNOWLEDGEMENTS

This work was supported by grants from the Canadian Institutes of Health Research (CIHR) to AM. and MP. AM was the recipient of a CIHR Investigator Award and currently holds a National Researcher Career Award from the Fonds de la Recherche en Santé du Québec. PES is supported by NIH grants R01-DK55758 and R01-CA112023 and is a recipient of an Irma T. Hirschl Career Scientist Award. PD, CC-B and PF were supported by studentships from the Canadian Diabetes Association and CIHR. KB and MET were supported by fellowships from Merck Frosst Inc. and the American Diabetes Association, respectively. We thank Geneviève Pilon for her contribution to the design of many experiments, as well as Luce Dombrowski and Natalie Lefort for technical assistance. We also thank Drs F. Picard and J. Lavoie for providing cells and plasmids.

## REFERENCES

1. Lehmann JM, Moore LB, Smith-Oliver TA, Wilkison WO, Willson TM, Kliewer SA: An antidiabetic thiazolidinedione is a high affinity ligand for peroxisome proliferator-activated receptor gamma (PPAR gamma). *J Biol Chem* 270:12953-12956, 1995
2. Yki-Jarvinen H: Thiazolidinediones. *N Engl J Med* 351:1106-1118, 2004
3. Bouskila M, Pajvani UB, Scherer PE: Adiponectin: a relevant player in PPARgamma-agonist-mediated improvements in hepatic insulin sensitivity? *Int J Obes Relat Metab Disord* 29 Suppl 1:S17-23, 2005
4. Combs TP, Pajvani UB, Berg AH, Lin Y, Jelicks LA, Laplante M, Nawrocki AR, Rajala MW, Parlow AF, Cheeseboro L, Ding YY, Russell RG, Lindemann D, Hartley A, Baker GR, Obici S, Deshaies Y, Ludgate M, Rossetti L, Scherer PE: A transgenic mouse with a deletion in the collagenous domain of adiponectin displays elevated circulating adiponectin and improved insulin sensitivity. *Endocrinology* 145:367-383, 2004
5. Pajvani UB, Du X, Combs TP, Berg AH, Rajala MW, Schulthess T, Engel J, Brownlee M, Scherer PE: Structure-function studies of the adipocyte-secreted hormone Acrp30/adiponectin. Implications for metabolic regulation and bioactivity. *J Biol Chem* 278:9073-9085, 2003
6. Nawrocki AR, Rajala MW, Tomas E, Pajvani UB, Saha AK, Trumbauer ME, Pang Z, Chen AS, Ruderman NB, Chen H, Rossetti L, Scherer PE: Mice lacking adiponectin show decreased hepatic insulin sensitivity and reduced responsiveness to peroxisome proliferator-activated receptor gamma agonists. *J Biol Chem* 281:2654-2660, 2006
7. Pajvani UB, Hawkins M, Combs TP, Rajala MW, Doebber T, Berger JP, Wagner JA, Wu M, Knopps A, Xiang AH, Utzschneider KM, Kahn SE, Olefsky JM, Buchanan TA, Scherer PE: Complex distribution, not absolute amount of adiponectin, correlates with thiazolidinedione-mediated improvement in insulin sensitivity. *J Biol Chem* 279:12152-12162, 2004
8. Waki H, Yamauchi T, Kamon J, Ito Y, Uchida S, Kita S, Hara K, Hada Y, Vasseur F, Froguel P, Kimura S, Nagai R, Kadowaki T: Impaired multimerization of human adiponectin mutants associated with diabetes. Molecular structure and multimer formation of adiponectin. *J Biol Chem* 278:40352-40363, 2003
9. Kahn BB, Alquier T, Carling D, Hardie DG: AMP-activated protein kinase: ancient energy gauge provides clues to modern understanding of metabolism. *Cell Metab* 1:15-25, 2005
10. Hotamisligil GS, Arner P, Caro JF, Atkinson RL, Spiegelman BM: Increased adipose tissue expression of tumor necrosis factor-alpha in human obesity and insulin resistance. *J Clin Invest* 95:2409-2415, 1995
11. Pickup JC, Mattock MB, Chusney GD, Burt D: NIDDM as a disease of the innate immune system: association of acute-phase reactants and interleukin-6 with metabolic syndrome X. *Diabetologia* 40:1286-1292, 1997
12. Chinetti G, Fruchart JC, Staels B: Peroxisome proliferator-activated receptors (PPARs): nuclear receptors at the crossroads between lipid metabolism and inflammation. *Inflamm Res* 49:497-505, 2000
13. Miles PD, Romeo OM, Higo K, Cohen A, Razaat K, Olefsky JM: TNF-alpha-induced insulin resistance in vivo and its prevention by troglitazone. *Diabetes* 46:1678-1683, 1997

14. Moller DE, Berger JP: Role of PPARs in the regulation of obesity-related insulin sensitivity and inflammation. *Int J Obes Relat Metab Disord* 27 Suppl 3:S17-21, 2003
15. Ricote M, Li AC, Willson TM, Kelly CJ, Glass CK: The peroxisome proliferator-activated receptor-gamma is a negative regulator of macrophage activation. *Nature* 391:79-82, 1998
16. Maggi LB, Jr., Sadeghi H, Weigand C, Scarim AL, Heitmeier MR, Corbett JA: Anti-inflammatory actions of 15-deoxy-delta 12,14-prostaglandin J2 and troglitazone: evidence for heat shock-dependent and -independent inhibition of cytokine-induced inducible nitric oxide synthase expression. *Diabetes* 49:346-355, 2000
17. Pilon G, Dallaire P, Marette A: Inhibition of inducible nitric-oxide synthase by activators of AMP-activated protein kinase: a new mechanism of action of insulin-sensitizing drugs. *J Biol Chem* 279:20767-20774, 2004
18. Perreault M, Marette A: Targeted disruption of inducible nitric oxide synthase protects against obesity-linked insulin resistance in muscle. *Nat Med* 7:1138-1143, 2001
19. Shimabukuro M, Ohneda M, Lee Y, Unger RH: Role of nitric oxide in obesity-induced beta cell disease. *J Clin Invest* 100:290-295, 1997
20. Zhou YT, Grayburn P, Karim A, Shimabukuro M, Higa M, Baetens D, Orci L, Unger RH: Lipotoxic heart disease in obese rats: implications for human obesity. *Proc Natl Acad Sci U S A* 97:1784-1789, 2000
21. Bedard S, Marcotte B, Marette A: Cytokines modulate glucose transport in skeletal muscle by inducing the expression of inducible nitric oxide synthase. *Biochem J* 325 ( Pt 2):487-493, 1997
22. Kapur S, Bedard S, Marcotte B, Cote CH, Marette A: Expression of nitric oxide synthase in skeletal muscle: a novel role for nitric oxide as a modulator of insulin action. *Diabetes* 46:1691-1700, 1997
23. Noronha BT, Li JM, Wheatcroft SB, Shah AM, Kearney MT: Inducible nitric oxide synthase has divergent effects on vascular and metabolic function in obesity. *Diabetes* 54:1082-1089, 2005
24. Fujimoto M, Shimizu N, Kunii K, Martyn JA, Ueki K, Kaneki M: A role for iNOS in fasting hyperglycemia and impaired insulin signaling in the liver of obese diabetic mice. *Diabetes* 54:1340-1348, 2005
25. Sugita H, Fujimoto M, Yasukawa T, Shimizu N, Sugita M, Yasuhara S, Martyn JA, Kaneki M: Inducible nitric-oxide synthase and NO donor induce insulin receptor substrate-1 degradation in skeletal muscle cells. *J Biol Chem* 280:14203-14211, 2005
26. Engeli S, Janke J, Gorzelniak K, Bohnke J, Ghose N, Lindschau C, Luft FC, Sharma AM: Regulation of the nitric oxide system in human adipose tissue. *J Lipid Res* 45:1640-1648, 2004
27. Torres SH, De Sanctis JB, de LBM, Hernandez N, Finol HJ: Inflammation and nitric oxide production in skeletal muscle of type 2 diabetic patients. *J Endocrinol* 181:419-427, 2004
28. Shibuya A, Wada K, Nakajima A, Saeki M, Katayama K, Mayumi T, Kadowaki T, Niwa H, Kamisaki Y: Nitration of PPARgamma inhibits ligand-dependent translocation into the nucleus in a macrophage-like cell line, RAW 264. *FEBS Lett* 525:43-47, 2002
29. Scherer PE, Williams S, Fogliano M, Baldini G, Lodish HF: A novel serum protein similar to C1q, produced exclusively in adipocytes. *J Biol Chem* 270:26746-26749, 1995

30. Peyrot ML, Nolan CJ, Soni K, Joly E, Lussier R, Corkey BE, Wang SP, Mitchell GA, Prentki M: Hormone-sensitive lipase has a role in lipid signaling for insulin secretion but is nonessential for the incretin action of glucagon-like peptide 1. *Diabetes* 53:1733-1742, 2004
31. Cho H, Mu J, Kim JK, Thorvaldsen JL, Chu Q, Crenshaw EB, 3rd, Kaestner KH, Bartolomei MS, Shulman GI, Birnbaum MJ: Insulin resistance and a diabetes mellitus-like syndrome in mice lacking the protein kinase Akt2 (PKB beta). *Science* 292:1728-1731, 2001
32. Tomas E, Tsao TS, Saha AK, Murrey HE, Zhang Cc C, Itani SI, Lodish HF, Ruderman NB: Enhanced muscle fat oxidation and glucose transport by ACRP30 globular domain: acetyl-CoA carboxylase inhibition and AMP-activated protein kinase activation. *Proc Natl Acad Sci U S A* 99:16309-16313, 2002
33. Yamauchi T, Kamon J, Minokoshi Y, Ito Y, Waki H, Uchida S, Yamashita S, Noda M, Kita S, Ueki K, Eto K, Akanuma Y, Froguel P, Foufelle F, Ferre P, Carling D, Kimura S, Nagai R, Kahn BB, Kadowaki T: Adiponectin stimulates glucose utilization and fatty-acid oxidation by activating AMP-activated protein kinase. *Nat Med* 8:1288-1295, 2002
34. Park SH, Gammon SR, Knippers JD, Paulsen SR, Rubink DS, Winder WW: Phosphorylation-activity relationships of AMPK and acetyl-CoA carboxylase in muscle. *J Appl Physiol* 92:2475-2482, 2002
35. Lessard SJ, Rivas DA, Chen ZP, Bonen A, Febbraio MA, Reeder DW, Kemp BE, Yaspelkis BB, 3rd, Hawley JA: Tissue-specific effects of rosiglitazone and exercise in the treatment of lipid-induced insulin resistance. *Diabetes* 56:1856-1864, 2007
36. Adams M, Reginato MJ, Shao D, Lazar MA, Chatterjee VK: Transcriptional activation by peroxisome proliferator-activated receptor gamma is inhibited by phosphorylation at a consensus mitogen-activated protein kinase site. *J Biol Chem* 272:5128-5132, 1997
37. Hu E, Kim JB, Sarraf P, Spiegelman BM: Inhibition of adipogenesis through MAP kinase-mediated phosphorylation of PPARgamma. *Science* 274:2100-2103, 1996
38. Guan Y, Hao C, Cha DR, Rao R, Lu W, Kohan DE, Magnuson MA, Redha R, Zhang Y, Breyer MD: Thiazolidinediones expand body fluid volume through PPARgamma stimulation of ENaC-mediated renal salt absorption. *Nat Med* 11:861-866, 2005
39. Zhang H, Zhang A, Kohan DE, Nelson RD, Gonzalez FJ, Yang T: Collecting duct-specific deletion of peroxisome proliferator-activated receptor gamma blocks thiazolidinedione-induced fluid retention. *Proc Natl Acad Sci U S A* 102:9406-9411, 2005
40. Singh S, Loke YK, Furberg CD: Long-term risk of cardiovascular events with rosiglitazone: a meta-analysis. *Jama* 298:1189-1195, 2007
41. Chakrabarti R, Vikramadithyan RK, Misra P, Hiriyan J, Raichur S, Damarla RK, Gershon C, Suresh J, Rajagopalan R: Ragaglitazar: a novel PPAR alpha PPAR gamma agonist with potent lipid-lowering and insulin-sensitizing efficacy in animal models. *Br J Pharmacol* 140:527-537, 2003
42. Cohen SE, Tseng YH, Michael MD, Kahn CR: Effects of insulin-sensitising agents in mice with hepatic insulin resistance. *Diabetologia* 47:407-411, 2004
43. Watkins SM, Reifsnyder PR, Pan HJ, German JB, Leiter EH: Lipid metabolome-wide effects of the PPARgamma agonist rosiglitazone. *J Lipid Res* 43:1809-1817, 2002

44. Wilson-Fritch L, Nicoloso S, Chouinard M, Lazar MA, Chui PC, Leszyk J, Straubhaar J, Czech MP, Corvera S: Mitochondrial remodeling in adipose tissue associated with obesity and treatment with rosiglitazone. *J Clin Invest* 114:1281-1289, 2004
45. Jiang G, Dallas-Yang Q, Li Z, Szalkowski D, Liu F, Shen X, Wu M, Zhou G, Doebber T, Berger J, Moller DE, Zhang BB: Potentiation of insulin signaling in tissues of Zucker obese rats after acute and long-term treatment with PPAR $\gamma$  agonists. *Diabetes* 51:2412-2419, 2002
46. Hevener AL, He W, Barak Y, Le J, Bandyopadhyay G, Olson P, Wilkes J, Evans RM, Olefsky J: Muscle-specific Pparg deletion causes insulin resistance. *Nat Med* 9:1491-1497, 2003
47. Gavrilova O, Haluzik M, Matsusue K, Cutson JJ, Johnson L, Dietz KR, Nicol CJ, Vinson C, Gonzalez FJ, Reitman ML: Liver peroxisome proliferator-activated receptor gamma contributes to hepatic steatosis, triglyceride clearance, and regulation of body fat mass. *J Biol Chem* 278:34268-34276, 2003
48. Kim JK, Fillmore JJ, Gavrilova O, Chao L, Higashimori T, Choi H, Kim HJ, Yu C, Chen Y, Qu X, Haluzik M, Reitman ML, Shulman GI: Differential effects of rosiglitazone on skeletal muscle and liver insulin resistance in A-ZIP/F-1 fatless mice. *Diabetes* 52:1311-1318, 2003
49. Chawla A, Schwarz EJ, Dimaculangan DD, Lazar MA: Peroxisome proliferator-activated receptor (PPAR) gamma: adipose-predominant expression and induction early in adipocyte differentiation. *Endocrinology* 135:798-800, 1994
50. Vidal-Puig AJ, Considine RV, Jimenez-Linan M, Werman A, Pories WJ, Caro JF, Flier JS: Peroxisome proliferator-activated receptor gene expression in human tissues. Effects of obesity, weight loss, and regulation by insulin and glucocorticoids. *J Clin Invest* 99:2416-2422, 1997
51. Brun RP, Kim JB, Hu E, Spiegelman BM: Peroxisome proliferator-activated receptor gamma and the control of adipogenesis. *Curr Opin Lipidol* 8:212-218, 1997
52. Kondo E, Sugiyama T, Kusaka H, Toyoda N: Adiponectin mRNA levels in parametrial adipose tissue and serum adiponectin levels are reduced in mice during late pregnancy. *Horm Metab Res* 36:465-469, 2004
53. Rangwala SM, Rhoades B, Shapiro JS, Rich AS, Kim JK, Shulman GI, Kaestner KH, Lazar MA: Genetic modulation of PPAR $\gamma$  phosphorylation regulates insulin sensitivity. *Dev Cell* 5:657-663, 2003
54. Kobayashi H, Ouchi N, Kihara S, Walsh K, Kumada M, Abe Y, Funahashi T, Matsuzawa Y: Selective suppression of endothelial cell apoptosis by the high molecular weight form of adiponectin. *Circ Res* 94:e27-31, 2004
55. Wulster-Radcliffe MC, Ajuwon KM, Wang J, Christian JA, Spurlock ME: Adiponectin differentially regulates cytokines in porcine macrophages. *Biochem Biophys Res Commun* 316:924-929, 2004
56. Yokota T, Oritani K, Takahashi I, Ishikawa J, Matsuyama A, Ouchi N, Kihara S, Funahashi T, Tenner AJ, Tomiyama Y, Matsuzawa Y: Adiponectin, a new member of the family of soluble defense collagens, negatively regulates the growth of myelomonocytic progenitors and the functions of macrophages. *Blood* 96:1723-1732, 2000
57. Thieringer R, Fenyk-Melody JE, Le Grand CB, Shelton BA, Detmers PA, Somers EP, Carbin L, Moller DE, Wright SD, Berger J: Activation of peroxisome proliferator-activated

receptor gamma does not inhibit IL-6 or TNF-alpha responses of macrophages to lipopolysaccharide in vitro or in vivo. *J Immunol* 164:1046-1054, 2000

58. Sripalakit P, Neamhom P, Saraphanchotiwitthaya A: High-performance liquid chromatographic method for the determination of pioglitazone in human plasma using ultraviolet detection and its application to a pharmacokinetic study. *J Chromatogr B Analyt Technol Biomed Life Sci* 843:164-169, 2006

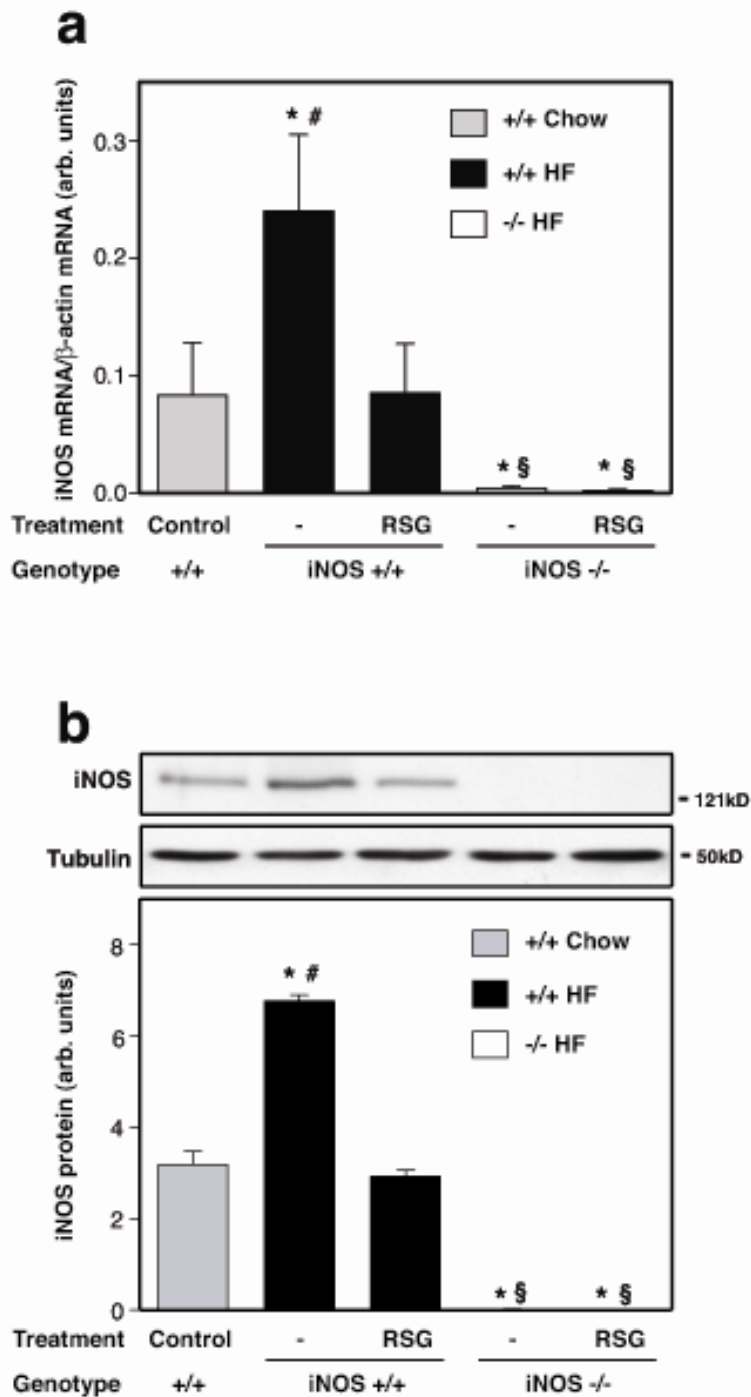
**Table 1**

Table I : Physiological parameters of iNOS<sup>+/+</sup> and iNOS<sup>-/-</sup> mice fed chow or high-fat diet and treated or not with RSG.

	iNOS <sup>+/+</sup> chow		iNOS <sup>-/-</sup> chow		iNOS <sup>+/+</sup> high fat		iNOS <sup>-/-</sup> high fat	
	Untreated	Rosi	Untreated	Rosi	Untreated	Rosi	Untreated	Rosi
Age (days)	167±1	166±1	167±1	164±1	162±1	163±1	163±1	163±1
Caloric intake (kCal/day)	139±05	150±04	135±10	147±08	223±07	245±18	259±09 <sup>#</sup>	258±1.1 <sup>†</sup>
Body weight								
Final (g)	288±04	287±04	285±06	299±06	386±12	355±06	385±13	386±1.1
Gain (g)	86±06	93±06	75±07	98±06	187±14	154±09	189±14	182±1.1
Total body fat mass (%)	162±1.1	152±06	165±1.2	187±1.4	31.0±1.4	28.9±3.2	27.5±3.0	28.3±2.1
Retroperitoneal WAT (mg)	192±15	184±13	195±20	226±23	785±72	587±54*	1021±79 <sup>#</sup>	753±80*
Brown adipose tissue (mg)	97±5	113±5	89±6	139±10 <sup>#*</sup>	132±9	182±8*	123±12	167±9 <sup>†*</sup>
Plasma triglycerides (mg/ml)	0.39±0.05	0.37±0.04	0.36±0.05	0.34±0.06	0.41±0.05	0.37±0.08	0.34±0.03	0.25±0.02 <sup>†</sup>
Blood glucose (mmol/l)	65±0.3	59±0.2	59±0.2	59±0.2	8.2±0.3	7.4±0.2*	8.4±0.3	7.7±0.2*
Plasma insulin (ng/ml)	0.8±0.2	0.4±0.1	0.5±0.1	0.5±0.1	3.2±0.6	1.8±0.3*	2.2±0.3	2.1±0.3
Plasma leptin (ng/ml)	28±0.4	4.6±0.7	3.0±0.3	3.3±0.5	24.7±4.9	20.6±3.7	33.1±5.1	35.6±4.4 <sup>#</sup>

\*P<0.05 vs respective untreated mice, <sup>#</sup> P<0.05 vs respective iNOS<sup>+/+</sup> mice, <sup>†</sup> P<0.05 vs respective diet untreated iNOS<sup>+/+</sup> mice (ANOVA analysis followed by Fisher's post hoc test)

**Figure 1**



**Fig. 1. RSG reduces iNOS expression in white adipose tissue of high fat-fed mice.** iNOS mRNA (a) and protein (b) expression was evaluated by semi-quantitative RT-PCR and western blotting in white adipose tissue of high fat (HF)-fed iNOS<sup>+/+</sup> and iNOS<sup>-/-</sup> mice and compared with chow-fed iNOS<sup>+/+</sup> mice. Each bar represents the mean  $\pm$  SE of 6-10 mice. Data are expressed as the ratio of iNOS over  $\beta$ -actin mRNA levels or as arbitrary units for iNOS protein. \* $P$ <0.05 vs untreated chow-fed iNOS<sup>+/+</sup>, # $P$ <0.05 vs respective RSG-treated mice, § $P$ <0.05 vs respective iNOS<sup>+/+</sup> mice.

**Figure 2**

Control

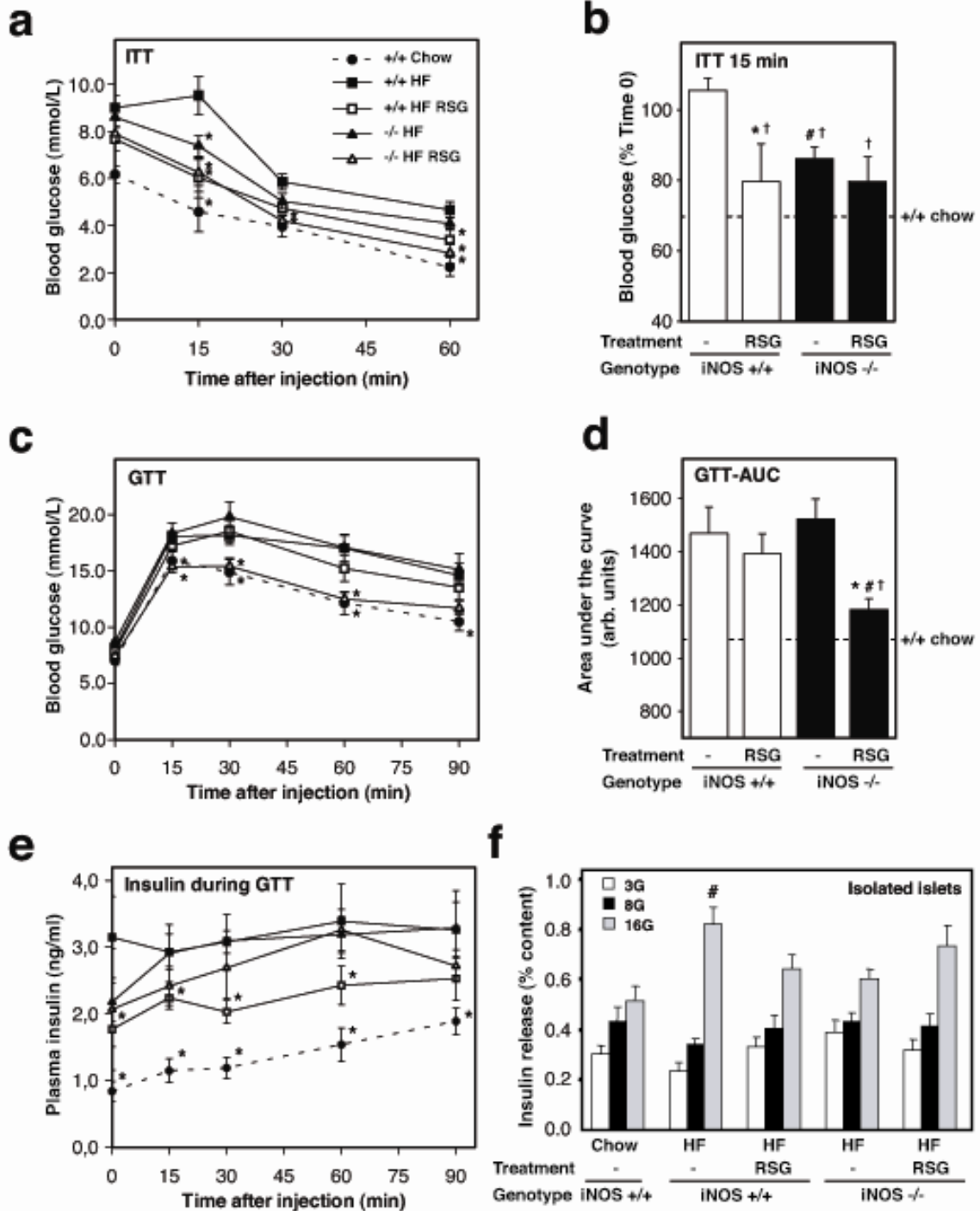


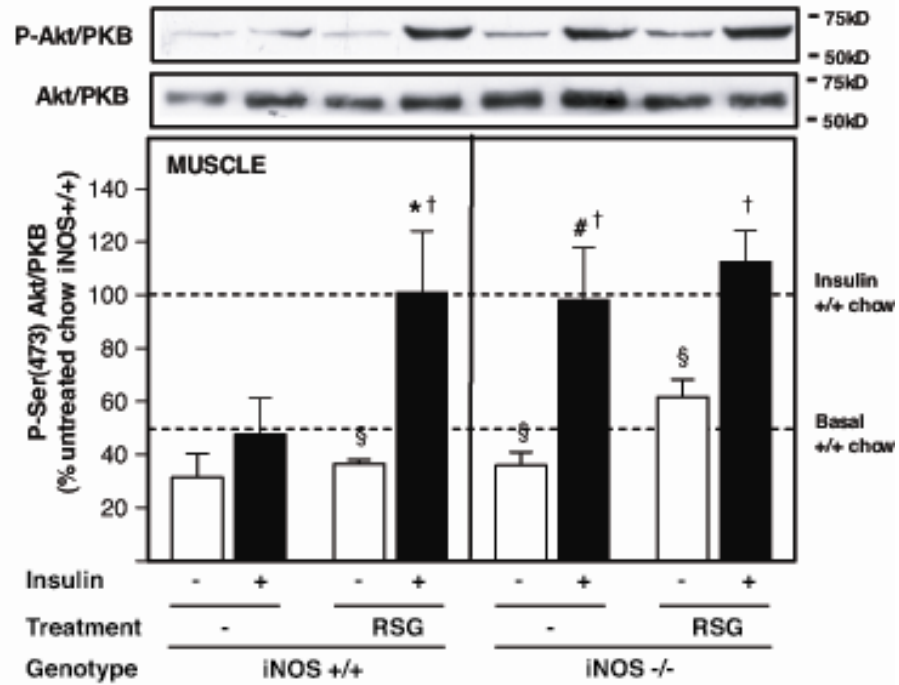
**fig. 2. Effect of iNOS gene disruption on the gluco-regulatory effects of RSG in high fat-fed obese mice. 5 h-fasted mice were acutely injected (i.p) with insulin (a-b) or**

*iNOS disruption sensitizes obese mice to PPAR $\gamma$  action*

glucose (**c-e**) and blood glucose (**a-d**) or plasma insulin (**e**) were measured at indicated times. Dashed lines represent values for untreated chow-fed iNOS<sup>+/+</sup> mice. (**a**) Insulin tolerance test (ITT) was performed for 60 min and relative blood glucose values at time 15 min was compared between groups (**b**). Glucose curves (**c**) and area under the curves (**d**) of a 90-min glucose tolerance test (GTT). Panel (**e**) shows plasma insulin concentrations during GTT. (**f**) Glucose-stimulated insulin release was measured in vitro using freshly isolated islets from 5 h-fasted mice at 3, 8, and 16 mM glucose (3G, 8G, 16G). Mean  $\pm$  SE of 6-10 mice per group. In (**a**), (**c**) and (**e**): \* $P < 0.05$  vs respective untreated high fat-fed iNOS<sup>+/+</sup> mice. In (**b**) and (**d**): \*  $P < 0.05$  vs untreated mice, # $P < 0.05$  vs iNOS<sup>+/+</sup> mice and † $P < 0.05$  vs untreated high fat-fed iNOS<sup>+/+</sup> mice. In (**f**): # $P < 0.05$  vs untreated chow-fed iNOS<sup>+/+</sup> mice.

**Figure 3**

**a**



**b**

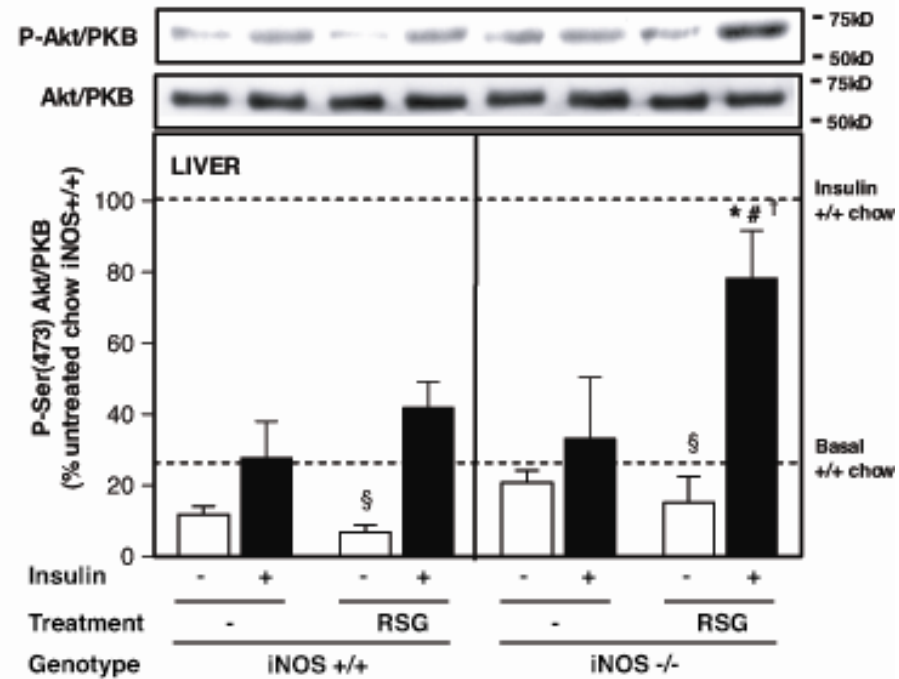
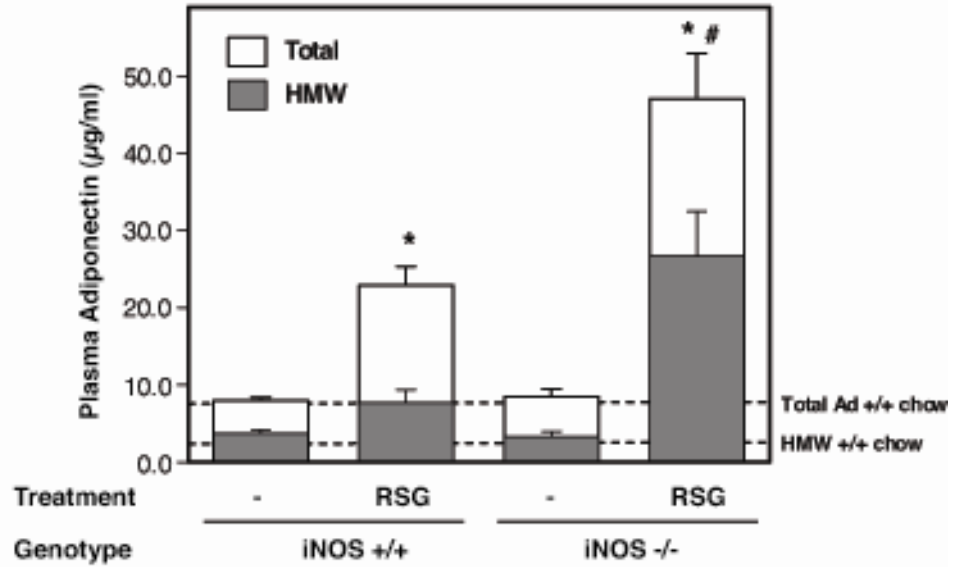


**Fig. 3. Effect of iNOS gene disruption and RSG on insulin-stimulated Akt phosphorylation in muscle and liver of high fat-fed obese mice.** Mice were acutely injected (i.v) with saline (open bars) or 3.8 U/kg insulin (black bars). Akt serine phosphorylation was evaluated 4 min after injection in quadriceps muscle (**a**) and liver (**b**) by western blot. Data are expressed relative to the mean values of insulin-stimulated, untreated chow-fed iNOS<sup>+/+</sup> mice (upper dashed line) loaded on the same gel. The lower dashed line represents basal Akt phosphorylation in untreated chow-fed iNOS<sup>+/+</sup> mice. Mean  $\pm$  SE of 3-5 mice per group. <sup>§</sup> $P < 0.05$  vs insulin-injected mice, \* $P < 0.05$  vs untreated mice, <sup>#</sup> $P < 0.05$  vs iNOS<sup>+/+</sup> mice, <sup>†</sup> $P < 0.05$  vs untreated high fat-fed iNOS<sup>+/+</sup> mice.

**Figure 4**

**a**



**b**

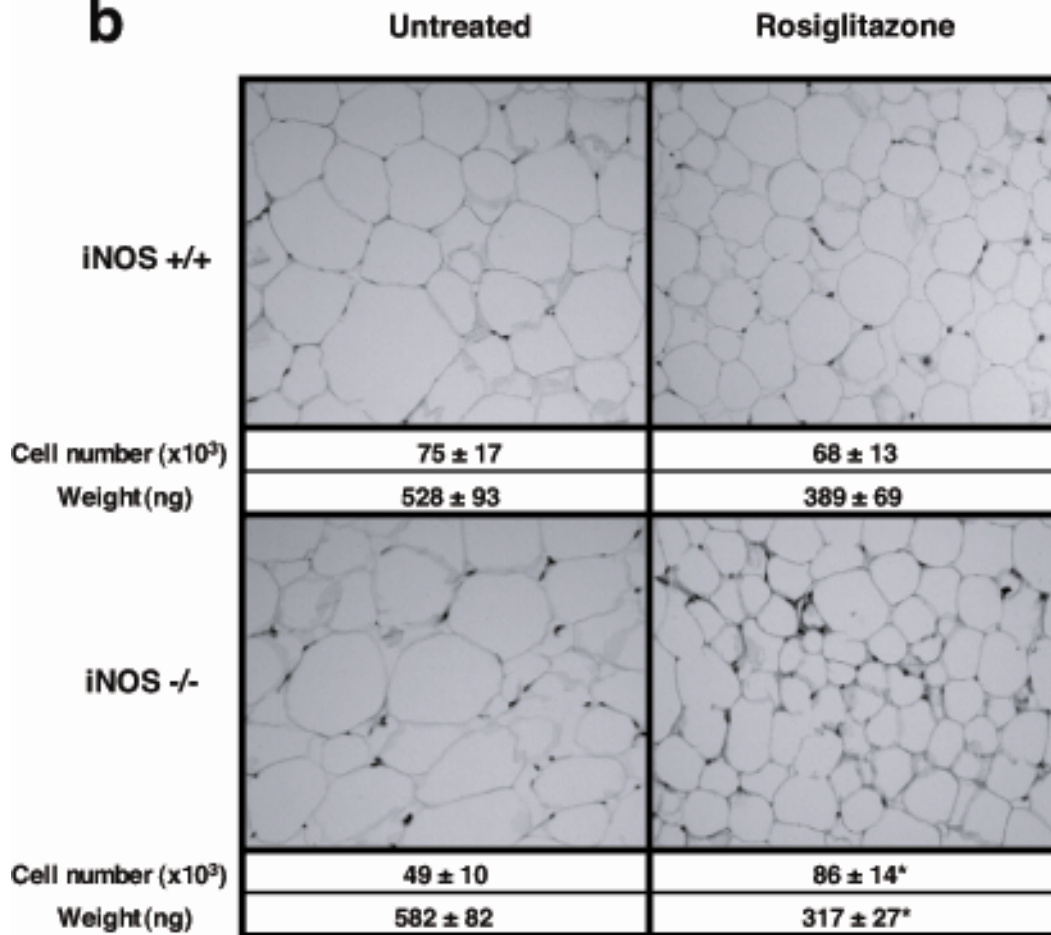


**Fig. 4. Effect of iNOS gene disruption and RSG treatment on plasma adiponectin and adipose tissue remodeling in high fat-fed obese mice.** (a) Total adiponectin concentrations (open bars) and high molecular weight adiponectin complexes (HMW, black bars) were measured in plasma by radioimmunoassay and size fractionation followed by quantitative western blotting, respectively. The dotted lines corresponds to total and HMW adiponectin levels in untreated chow-fed iNOS<sup>+/+</sup> mice. (b) Histological analysis of white adipose tissue of high fat-fed animals. Mean weight and cell number per fat pad are also shown. Bars represent the mean  $\pm$  SE of 5-16 mice per group. \* $P$ <0.05 vs untreated mice, # $P$ <0.05 vs iNOS<sup>+/+</sup> mice.

## Figure 5

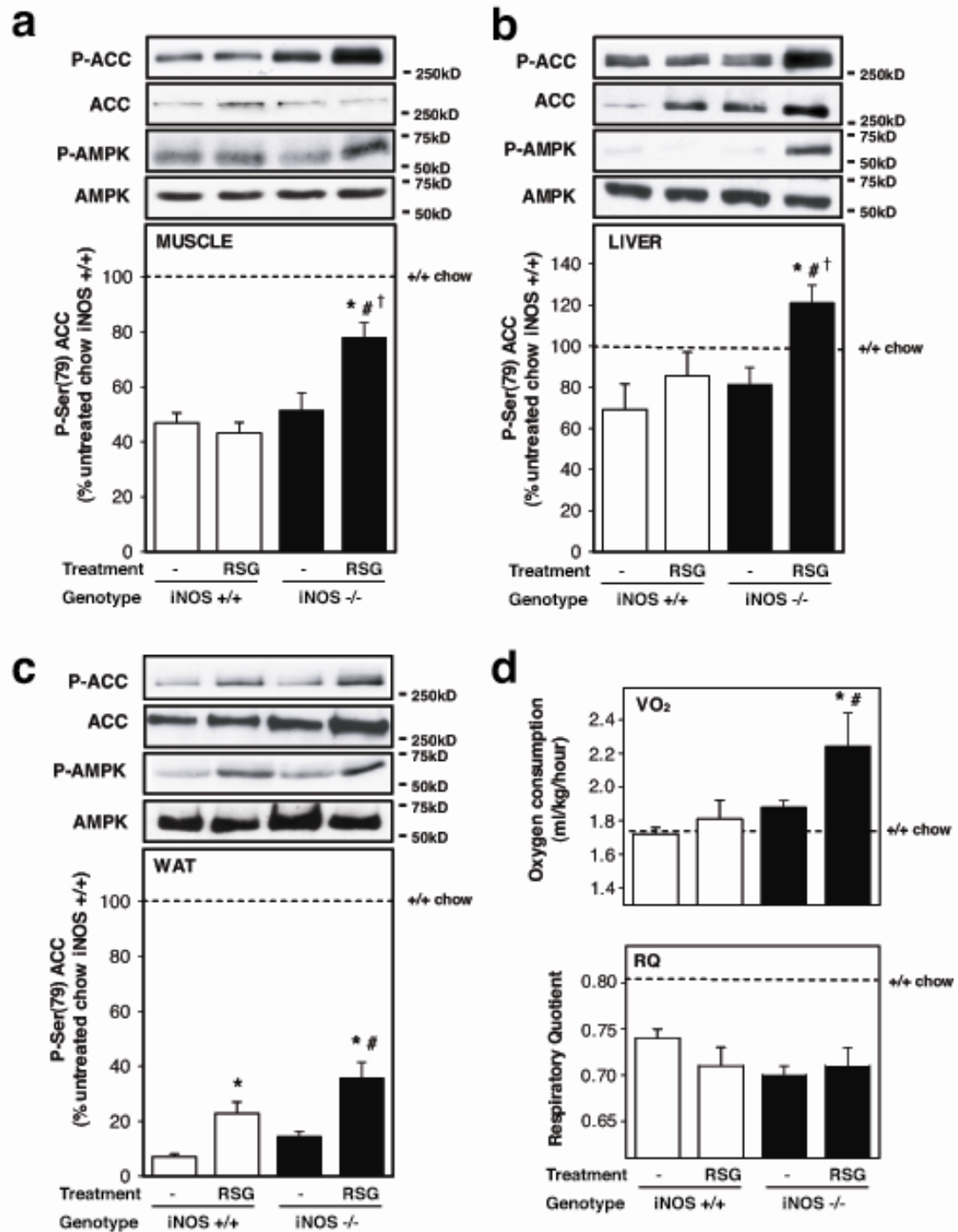


**Fig. 5. Effect of iNOS gene disruption and RSG treatment on AMPK activation and energy expenditure in high fat-fed mice.** Phosphorylation of AMP-activated kinase (P-AMPK) and acetyl-CoA carboxylase (P-ACC) as well as total expression were evaluated in

*iNOS disruption sensitizes obese mice to PPAR $\gamma$  action*

quadriceps muscle (**a**), liver (**b**) and white adipose tissue (**c**) by western blotting. Data are expressed relative to untreated chow-fed iNOS<sup>+/+</sup> mice values (dashed lines) analyzed on the same gels. Whole-body energy expenditure (**d**, upper panel) and respiratory quotient (RQ) (**d**, lower panel) were measured by indirect calorimetry. Mean  $\pm$  SE of 4-8 mice per group. \* $P$ <0.05 vs respective untreated mice, # $P$ <0.05 vs respective iNOS<sup>+/+</sup> mice, † $P$ <0.05 vs untreated high fat-fed iNOS<sup>+/+</sup> mice.

**Figure 6**

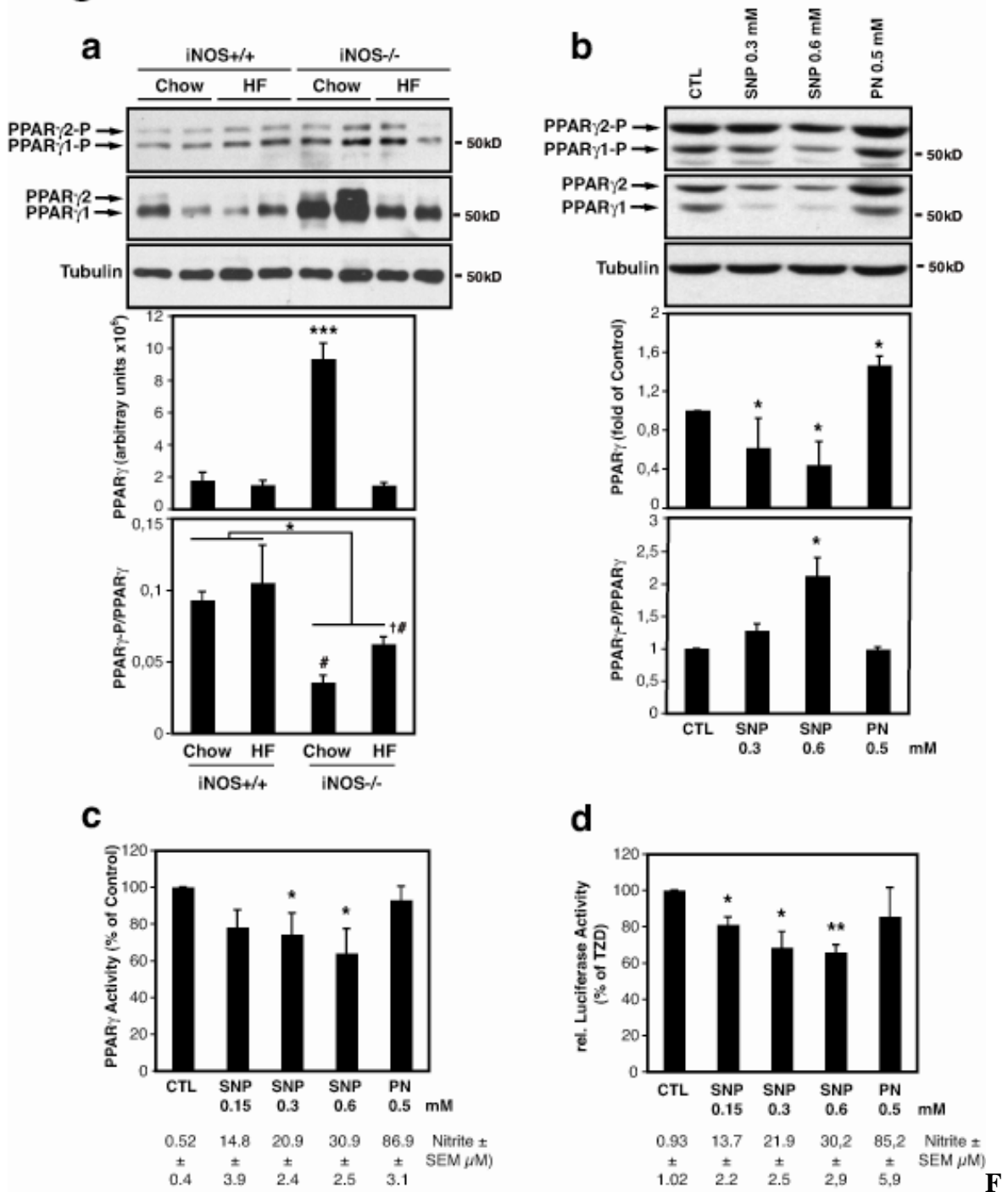


**fig. 6. The iNOS/NO pathway suppresses PPAR $\gamma$  activation.**

(a) White adipose tissue (WAT) extracts were analyzed by immunoblotting for PPAR $\gamma$  expression and phosphorylation on Ser-82/112, as well as for tubulin expression. Shown are representative gels and means  $\pm$  SE of 5 animals per group.  $P < 0.05$  (\*) or  $P < 0.001$

*iNOS disruption sensitizes obese mice to PPAR $\gamma$  action*

(\*\*\*), versus wild-type chow mice. <sup>#</sup> $P < 0.05$  vs respective iNOS<sup>+/+</sup> mice, <sup>†</sup> $P < 0.05$  vs untreated high fat-fed iNOS<sup>+/+</sup> mice. **(b, c)** Differentiated 3T3-L1 adipocytes were treated with sodium nitroprusside (SNP) or peroxyntirite (PN) at the indicated concentrations for 24 h. **(b)** Total cellular extracts were analyzed by western blot for the expression of PPAR $\gamma$  and its phosphorylation on Ser-82/112, as well as tubulin levels. **(c)** Nuclear extracts were analyzed for PPAR $\gamma$  activity, as described in Methods. Shown are means  $\pm$  SE of 4 determinations in two individual experiments; \*,  $P < 0.05$  versus control (CTL) cells. **(d)** Luciferase assays of 293T cells transfected with PPAR $\gamma$ 2 and pGL3-PPRE and treated with SNP or PN at the indicated concentration for 24 h. 20  $\mu$ M of troglitazone was added during the last 16 h of treatment. Shown are means  $\pm$  SE of 4 individual experiments done in triplicate; \*,  $P < 0.05$ , \*\*,  $P < 0.01$  versus control (CTL) cells. In (c) and (d), supernatants were sampled for nitrite determinations and values are shown under the graphs.

**Figure 7**

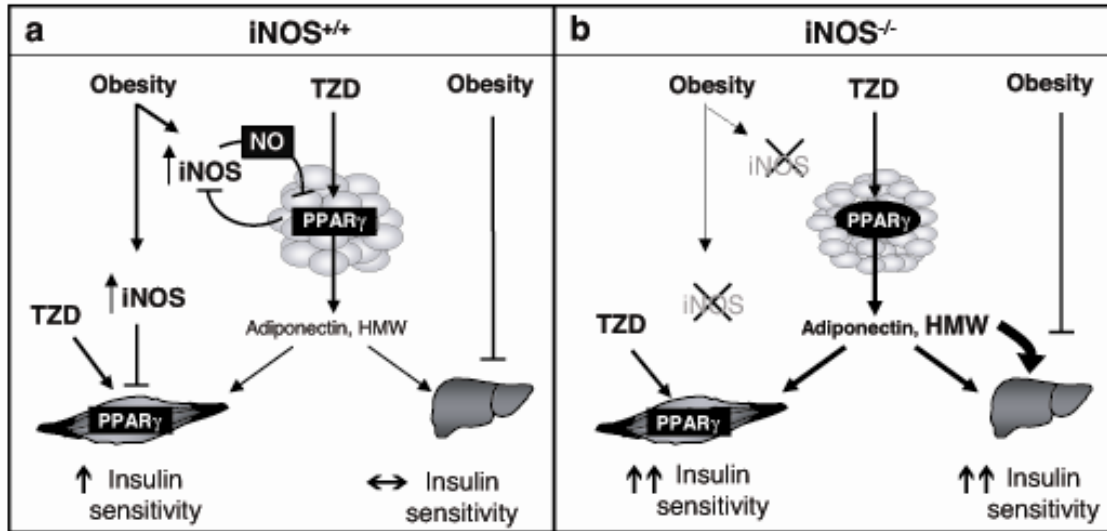


**Fig. 7. Proposed model by which iNOS induction in obesity modulates TZD/PPAR $\gamma$  agonism in insulin-target tissues.**

In wild-type  $iNOS^{+/+}$  mice (a), obesity leads to  $iNOS$  induction in fat and muscle, which contributes to promote insulin resistance in muscle and impairs PPAR $\gamma$  action in adipose tissue. Obesity also impairs hepatic insulin action even if  $iNOS$  is not induced, as shown in liver of high fat-fed obese mice (18). PPAR $\gamma$  agonists such as TZDs reduce  $iNOS$  induction in obese  $iNOS^{+/+}$  mice leading to improvement in insulin action in muscle but not in liver.  $iNOS$  disruption ( $iNOS^{-/-}$ ) (b) increases muscle insulin action but also sensitizes obese mice to the effect of PPAR $\gamma$  ligands on adipose tissue, leading to increased number of smaller adipocytes and enhanced secretion of adiponectin, particularly in its HMW complex form. Elevated HMW adiponectin mainly targets the liver through AMPK activation, resulting in increased hepatic insulin action and improved glucose tolerance.